Published in final edited form as:
Atherosclerosis. 2011 June ; 216(2): 283–291. doi:10.1016/j.atherosclerosis.2011.02.036.

Simvastatin preserves diastolic function in experimental hypercholesterolemia independently of its lipid lowering effect

Dallit Mannheim[a,1], **Joerg Herrmann**[a,1], **Piero O. Bonetti**[b], **Ronit Lavi**[c], **Lilach O. Lerman**[a,c], and **Amir Lerman**[a,*]

[a] Division of Cardiovascular Diseases, Mayo Clinic, Rochester, MN, USA [b] Division of Cardiology, Kantonsspital Graubuenden, Chur, Switzerland [c] Division of Nephrology and Hypertension, Mayo Clinic, Rochester, MN, USA

Abstract

Objective: Isolated diastolic dysfunction is present in 40% of heart failure patients. It has been attributed to myocardial fibrosis and related to cardiovascular risk factor exposure. We hypothesized that simvastatin will improve these dynamics in experimental hypercholesterolemia (HC).

Methods: Three groups of pigs were studied after 12 weeks of normal (N) diet, HC diet, or HC diet with simvastatin (80 mg/day) treatment. Cardiac function was assessed by electron beam computed tomography (EBCT) and percentage of myocardium occupied by microvessels (myocardial vascular fraction) was calculated by micro-CT. Collagen content was determined by Sirius red staining and confirmed by a quantitative, hydroxyoproline-based assay.

Results: Compared with N, LDL serum concentration was higher in HC and HC + simvastatin (1.0 ± 0.1 vs. 7.9 ± 1.7 and 9.6 ± 1.2 mmol/L, $p < 0.05$ for both). Cardiac early diastolic filling was reduced in HC compared with N (102.4 ± 11.3 vs. 151.1 ± 12.1 mL/s; $p < 0.05$) but restored in HC + simvastatin (176.8 ± 21.3 mL/s, $p < 0.05$ vs. HC). Compared with N, myocardial vascular fraction was higher in HC but not in HC + simvastatin (1.98 ± 0.84 vs. 4.48 ± 0.31 and 2.95 ± 0.95%; $p < 0.05$ for HC vs. N). Myocardial collagen content was higher in HC than in HC + simvastatin and N (4.72 ± 1.03 vs. 1.62 ± 0.12 and 1.21 ± 0.24% area staining; $p < 0.05$ for HC vs. N), which was attributable mainly to an increase in collagen III (2.90 ± 0.48 vs. 1.62 ± 0.12 and 1.21 ± 0.24% area staining; $p < 0.05$ for HC vs. N).

Conclusions: Simvastatin is able to prevent diastolic dysfunction in experimental HC independent of its lipid lowering effect. This beneficial effect is, at least partially, due to a decrease in myocardial fibrosis and angiogenesis.

Keywords

Diastolic dysfunction; Hypercholesterolemia; Fibrosis; Angiogenesis

* Corresponding author at: Division of Cardiovascular Diseases, Mayo Clinic Rochester, 200 First Street SW, Rochester, MN 55905, USA. Tel.: +1 507 255 4152; fax: +1 507 255 2550. lerman.amir@mayo.edu (A. Lerman)..

[1] Both authors contributed equally to this manuscript.

Disclosure

None.

1. Introduction

Diastolic dysfunction of the heart refers to the impairment of the filling of the ventricles with an adequate volume of blood due to a decrease in relaxation properties and/or increase in ventricular stiffness [1]. This condition can lead to signs and symptoms of heart failure even in the absence of any impairment in systolic function, justifying the clinical diagnosis of isolated diastolic heart failure in 40–50% of all patients diagnosed with heart failure [2]. Even though the average mortality rate has been considered to be lower with diastolic than with systolic heart failure, 20–25% of all patients with moderate-to-severe diastolic dysfunction will not survive 5 years [2]. Thus, diastolic dysfunction poses a significant health care burden and calls for attentive medical therapy.

A number of different pathophysiological mechanisms have been considered to contribute to the development of diastolic dysfunction [3]. Changes in the composition of the extracellular matrix are of crucial significance, especially quantitative and qualitative alterations of fibrillar collagen [4], These include increase in the total amount of collagen, the ratio of type I collagen to type III collagen, and collagen cross-linking. Collagen synthesis is controlled by various mechanical and biochemical factors such as local blood pressure, the renin–angiotensin–aldosterone system (RAAS), and growth factors such as transforming growth factor (TGF)-β_1 [5], Stimulation of RAAS has also been linked to increased reactive oxygen species (ROS) production, which activates not only the TGF-β_1 pathway but also leads to a reduction in the bioavailability of nitric oxide (NO), an important factor for the modulation of ventricular relaxation and stiffness [6]. Thus, advances have been made to unravel the mechanisms for the development of diastolic heart failure and indicated areas of intriguing overlap with vascular biology.

HMG-CoA-reductase inhibitors, commonly referred to as “statins”, were introduced into clinical practice to lower serum cholesterol levels [8]. The clinical benefit seen with this class of drugs, however, clearly outweighs any lipid-lowering effect. For this reason, non-lipid-lowering or pleiotropic effects were proposed and eventually confirmed in a number of studies, mainly in the vascular biology sector [8]. These include increase in the expression and activity of endothelial NO synthase (eNOS) and a decrease in RAAS function and NADPH oxidase activity, one of the major sources of ROS production [7]. Considering these effects, one may speculate on a beneficial impact of statins on diastolic dysfunction. Indeed, two clinical studies suggested that statins significantly prolong survival of patients with diastolic heart failure [9, 10]. However, the mechanisms underlying these clinical benefits and the relative contribution of the lipid-lowering effects have remained unknown.

Porcine experimental hypercholesterolemia (HC) is an established model of vascular disease and is associated with an increase in vasa vasorum spatial density and vascular collagen content as well as a decrease in vascular NO bioavailability, endothelium-dependent relaxation properties, and myocardial perfusion [11]. Intriguingly, these changes are prevented by simvastatin and not related to its lipid-lowering effects [12, 13]. Even though HC has been associated with cardiac dysfunction in clinical studies, particularly diastolic dysfunction, experimental evidence for this association has remained scarce and no experimental study has yet investigated the impact of statin therapy on diastolic function in this setting independent from any lipid-lowering effects. This was the primary objective of the current study.

2. Materials and methods

2.1. Animals

All procedures were approved by the Institutional Animal Care and Use Committee and conform to the *Guide for the Care and Use of Laboratory Animals* published by the US National Institutes of Health (NIH Publication No. 85-23, revised 1996). Three groups (n = 6 each) offemale, non-ovariectomized domestic pigs (55–65kg, 6 months of age) were studied after 12 weeks of normal diet (N) or HC diet (HC; 2% cholesterol and 15% lard by weight; TD93296, Herlan Teklad) or HC diet + simvastatin (HC + simv; initially 40mg/day increased to 80mg/day after 5 weeks, taken with the feed). The dosing was based on our previous studies [13, 14]. Plasma lipid profile (preformed by spectrophotometry, Roche, Nutley, NJ) as well as in vivo measurements of LV function, vascular resistance and muscle mass (using electron beam computed tomography (EBCT)), were performed after twelve weeks. Animals were then euthanized with intravenous pentobarbital (20 cm^3 of Sleepaway®, Fort Dodge Laboratories, Fort Dodge, IA). The heart was immediately removed and prepared for microtomographic analysis of the myocardial microvessels, as previously described [15]. In addition, transmural blocks of myocardium from the anterior left-ventricular wall (1–2 cm in length) were flash-frozen in liquid nitrogen for western blotting or were fixated in formalin for paraffin imbedding and histological studies.

2.2. Electron beam computed tomography

EBCT (Imatron c-150, Imatron Inc., South San Francisco, California) was used for in vivo assessment of LV function and myocardial vascular resistance as well as LV muscle mass (LVMM) to exclude LV hypertrophy, as previously described [16, 17].

Briefly, the animals were anesthetized with IM ketamine and xylazine (20 mg/kg and 2 mg/kg, respectively, with a maintenance dose of intravenous ketamine and xylazine 0.2 mg/kg and 0.03 mg/kg in saline), intubated and mechanically ventilated. Catheters were placed fluoroscopically in the aorta, for measurement of mean arterial pressure (MAP), and in the right atrium for contrast medium injections. Cross-sectional images at two adjacent mid-left ventricle levels were identified by localization scans. After abolus injection (0.3 ml/kg over 2s) of nonionic, low-osmolar contrast media iopamidol (Isovue-370, Squibb Diagnostics, Princeton, New Jersey), 40 consecutive electrocardiogram (ECG)-triggered end-diastolic scans were obtained over the selected levels at 1–3 heartbeat intervals. Ten to 15min after this baseline study a 10-min cardiac challenge with intra-venous adenosine was started, titrated to the maximal dose possible while maintaining hemodynamic stability (about 400 mcg/kg/min). Once EBCT scans were acquired, adenosine infusion was discontinued to a new testing state. Thereafter, ECG-triggered cine sequence with 8 mm-thick tomographic slices in the short axis from the LV apex through the base (overall 8 levels) were obtained during power injection of the contrast agent (4mL/s) and suspension of respiration. The images were reconstructed and analyzed using Analyze® software package (Biomedical Imaging Resource, Mayo Clinic, Rochester, MN) [14, 16]. The endocardial and epicardial borders were traced at end-diastole and end-systole allowing calculation of LV size, stroke volume, ejection fraction, and LVMM. For diastolic function, we calculated the LV volume at 16 points through the cardiac cycle and plotted it versus time [17]. Subsequently, the maximal positive slope during the rapid filling phase, which represents early diastolic filling rate, was calculated [18].

2.3. Microscropic computed tomography (micro–CT)

Hearts were prepared as previously described [15]. Briefly, the proximal left anterior descending artery was cannulated in situ and perfused with a solution of normal saline and heparin to flush out the remaining blood. An intravascular radiopaque microfil silicone

rubber (MV-122, Flow Tech, Inc, Carver, MA) was injected at a physiological perfusion pressure (100 mmHg)until it flowed freely from the myocardial veins. Atransmural portion of the LV (approximately 2cm × 1cm × 1cm) was sectioned and scanned [15].

The micro-CT scanner has been previously described [15], Myocardial samples were scanned using 0.5° angular increments, providing 721 views around 360°. Images were recorded, digitized, and transferred to a controlling computer. The 3D volume images consisted of cubic voxels 20μm on-a-side, and were displayed at this resolution. The radiopacity of each voxel was represented by a 16-bit gray-scale value.

Using Analyze® [15], the myocardium was three dimensionally oriented to obtain anatomically comparable samples for study. Subsequently, the myocardium was divided into two equal parts, classified as subendocardium and subepicardium.

Microvessels (diameters <500 μm) were measured in each tomographic section using the "Object Counter" function, and classified as either small (diameters between 40 and 100 μm) or large (diameters of 101–500 μm). Diameters of microvessels larger than 100 μm were measured manually. Microvessels smaller than 40 μm (<2 voxel) were excluded to avoid error due to noise and the average vessel diameter was calculated. The entire area of myocardium in each slice was traced and microvascular density (number of vessels per slice) and vascular volume fraction (percentage of the area of each slice occupied by the cross section area of the vessels) were calculated.

Using the “connectivity” function three intra-myocardial arteries and their branches were isolated in each pig. The vessel elongation factor (the total 3D distance divided by the shortest distance, between the epicardial vessel and the end point of the main branches), representing vessel tortuousity (typical for neovascularization), was calculated using “tree analysis” software.

2.4. Immunoblotting

Following removal of any necrotic edges, transmural cuts were taken from the frozen myocardial samples (200 mg on average) and homogenized using a standard lysis buffer as described before [12, 13]. Protein concentrations were calculated by Bradford assay (BioRad, CA). Equal amount of myocardial homogenate protein (100 μg) were dissolved in SDS–polyacrylamide gels and electrophoretically transferred onto nitrocellulose membranes (Bio-Rad, Hercules, CA). Membranes incubated overnight at 4°C with either anti-b-FGF (rabbit 1:100, Santa Cruz Biotechnology, Inc., CA) or anti-TGFβ_1 (rabbit 1:100, Santa Cruz Biotechnology, Inc., CA) as previously described [16, 17], Then the appropriate horseradish peroxidase-linked secondary antibody was used, and the proteins were detected by electrochemiluminescence. β-Actin was used as the loading control.

2.5. Immunostaining

As previously described, after deparaffinizing, hydrating, quenching endogenous peroxidase and blocking [16], anterior left-ventricular myocardial tissue sections were incubated overnight at 4°C with rabbit anti-VEGF-A (1:100, Santa-Cruz Biotechnology, Inc., CA) then for 30 min with the appropriate secondary antibody (Dako A/S, Glostrup, Denmark). Nova-red was used as chromogen. All sections were counterstained with Hematoxylin. Normal mouse immunoglobulin fraction was used as negative control.

Staining was visualized under a standard light microscope (Olympus, Leeds Precision Instruments). Pictures were taken with an imaging program (SPOT Advanced 3.3, Diagnostic Instruments Inc.) and analyzed using image analysis computer software (Meta-Morph, Meta Imaging Series 4.6). For the quantification, percent area staining was

calculated. This analysis was performed on two to three areas per one specimen slide per pig.

2.6. Sirius red staining

The interstitial collagen content of the myocardium was evaluated by Sirius red [17,19]. Specimen sections were deparaffinized, rehydrated and incubated with 0.1% Sirius red in saturated picric acid for 60 min, then 1% acetic acid for 30 min, counterstained in hematoxylin, differentiated in acid alcohol solution, rehydrated and mounted. Slides were visualized under both bright-field and polarized light microscope, and pictures of the entire slice were taken with identical exposure settings for all sections and analyzed using image analysis computer software (MetaMorph, Meta Imaging Series 4.6). Results were quantified as percent area staining.

The content of collagen, identified by birefringence under polarized light, was evaluated as percent of the tissue area. The use of polarized light furthermore allows the differentiation of collagen I and III. Collagen I thick fibers are seen as red/orange fibers under polarized light while collagen III thinner fibers are seen as yellow/green. These analyses were performed on two to three areas (except for only one area in one pig in the HC group) per one specimen slide per pig.

2.7. Total collagen and collagen cross linking

Total collagen, pepsin-soluble and pepsin insoluble (cross-linked) collagen were also quantified by measuring hydroxyproline using a modified Stegemann method [20]. Briefly, equal amount of LV tissue were homogenized and hydrolysed and incubated with chloramin/citrate acetate buffer with propanol at room temperature for 20min. Then Ehrlich's buffer was added and heated at 65°C for 30 min. The intensity of the red color that developed was measured by spectrophotometry and compared to the standard curve.

The myocardial pepsin-insoluble collagens were extracted by incubation for 24h with 5mg/mL pepsin in 0.5 mol/L acetic acid [21]. The soluble and insoluble collagens were separated by centrifugation and the hydroxyproline was measured in both the supernate and the pellet (after dissolving in water).

2.8. Data analysis

Two group comparisons were made by Student t-test for continuous variables or the χ^2 test for categorical variables. Multiple group comparisons were performed by ANOVA followed by Tukey–Kramer post-hoc analysis. Data were presented as percentage or mean ± SEM. Statistical significance was assumed for $p < 0.05$ for all analyses.

3. Results

3.1. Animals

After 12 weeks of HC diet, there was a significant increase in plasma cholesterol (total, low density lipoprotein, high density lipoprotein) in both groups of cholesterol-fed pigs (HC and HC + simv) compared with animals fed a normal diet (Table 1). There were no differences in mean arterial pressure and heart rate at baseline or in response to challenge with adenosine, nor were there any differences in systemic vascular resistance and LV muscle mass between the groups (Table 1).

3.2. EBCT imaging

Systolic function, as assessed by ejection fraction and cardiac output, was similar among the three study groups (Table 1). Diastolic function, as assessed by the diastolic filling rate, was significantly decreased in HC and was preserved in the HC + simv group (Table 1). While myocardial vascular resistance was similar in all groups at baseline (Table 1), myocardial vascular resistance response to challenge with adenosine was blunted in HC and preserved with the addition of simvastatin to the HC diet (Table 1). There was a strong correlation between diastolic filling rate and myocardial vascular resistance in response to adenosine challenge ($r = 0.69$, $p = 0.01$).

3.3. Micro-CT imaging

Fig. 1 illustrates the changes of the microvascular architecture of the myocardium. HC was associated with a significant increase in the number of microvessels per myocardial area (microvascular density) and vascular volume fraction (Table 2). Moreover, the tortuousity of the myocardial microvessels was noted to be increased in HC compared with N, which was completed prevented by simvastatin (vascular elongation factor 1.6 ± 0.0* vs. 1.3 ± 0.1 and 1.3 ± 0.1, $p < 0.05$). The addition of simvastatin to the HC diet also attenuated the increase in microvascular density and vascular volume fraction (Table 2). No significant difference between the groups was observed for the average diameter of larger microvessels (N, HC, and HC + simv: 67.6 ± 3.1, 57.1 ± 2.9, and 61.9 ± 7.2 μm, respectively).

3.4. Immunoblotting and immunostaining

Along with the neovascularization changes in HC, the expression of the pro-angiogenic factors b-FGF and VEGF-A was increased in HC and significantly decreased by concomitant simvastatin treatment (Fig. 2). Furthermore, there was a significant increase in the expression of TGF-β_1 in the myocardium of HC animals, which was attenuated by simvastatin (Fig. 3).

3.5. Sirius red staining and hydroxyproline assay

Compared to N, HC was associated with an increase in total collagen, collagen III and collagen cross-linking (insoluble collagen) (Figs. 4 and 5). This increase in collagen was observed predominantly in the perivascular area and to a lesser extent diffusely in the myocardium (Fig. 5, top). This increase in collagen was attenuated by the addition of sinvastatin to the HC diet (Fig. 5).

4. Discussion

The current study demonstrates (1) that experimental HC leads to neovascularization, a primarily perivascular increase in myocardial collagen content, and diastolic dysfunction and (2) that administration of simvastatin can prevent these changes in the absence of any significant lipid-lowering effect. These findings support the concept that HC contributes to diastolic dysfunction at least in part via angio-fibrotic remodeling. Interference with this process rather than reduction of lipid serum concentrations seems to be a key element of the beneficial effects of statins on myocardial function in this setting.

4.1. Diastolic function assessment with EBCT

Various non-invasive imaging techniques have been used to assess diastolic function. The most commonly used techniques are Doppler echocardiography, tissue Doppler echocardiography, magnetic resonance imaging, and radionuclide angiography [22]. With high temporal resolution (50 ms/image) that minimizes motion artifacts, EBCT allows time-dependent tracking of LV volume changes throughout the cardiac cycle and the

determination of peak-filling and peak-emptying rates and thereby a quantitative analysis of diastolic function [23]. Clinical studies in healthy individuals showed a good correlation between EBCT and contrast-enhanced echocardiography for the determination of end-diastolic and end-systolic ventricular volume, stroke volume, and ejection fraction [24]. Likewise in healthy individuals, the quantification of early diastolic filling by EBCT was verified by radionuclide angiography [25]. Subsequent studies furthermore confirmed this utilization of EBCT in patients with well-described abnormalities of diastolic function, for instance in the setting of myocardial ischemia and hypertrophic cardiomyopathy. In accordance with these human studies, we have been able to determine diastolic function in domestic pigs by EBCT as published before [17]. The main advantage of EBCT has been the use of a “one-stop” technique not only for the determination of cardiac function but also for the reliable quantification of myocardial perfusion and permeability [26,27]. In a prior study, we reported on the improvement of myocardial microvascular function in hypercholesterolemic pigs treated with simvastatin using EBCT [14]. The current study represents the extension of this study analyzing diastolic function in the same set of animals undergoing the same set of investigational procedures. Hence, even though not as widely used as other imaging techniques, EBCT can assess diastolic filling dynamics reliably well and was utilized in the current study in agreement with previous reports in domestic pigs subjected to HC and simvastatin treatment.

4.2. Diastolic dysfunction in HC

An inverse correlation between total and LDL cholesterol levels and diastolic function by standard echocardiographic parameters was first noted in hypertensive postmenopausal women [28]. Sub-sequently, it was observed that diastolic function is impaired in normotensive hyperlipidemic patients [29]. In a more controlled, experimental setting, Huang et al. were able to show that feeding rabbits a high-cholesterol diet leads to an impairment in calcium uptake into the sarcoplasmic reticulum within four days and impairment in systolic shortening and diastolic relaxation rates after ten weeks [30]. Moreover, Zhu et al. were able to demonstrate a significant decrease in the diastolic filling rate by EBCT in pigs fed a high-cholesterol diet for 12 weeks, which was inversely related to the extent of myocardial fibrosis as determined by Trichrome staining [17]. The current results consolidate these findings and furthermore show an increase in collagen cross-linking in HC, which has been considered to be at least as important as the increase in total collagen content for myocardial stiffness [31]. Of note, similar changes of perivascular fibrosis can be observed in pigs subjected to systemic arterial hypertension, the risk factor most widely linked with diastolic dysfunction [32]. Hence, various lines of evidence support the concept that HC leads to impairment in the relaxation and stiffness of the ventricle and hence diastolic dysfunction.

4.3. Mechanisms of diastolic dysfunction in HC

The first experimental study to demonstrate the development of diastolic dysfunction with HC also showed a preceding decrease in the expression of molecules centrally involved in intra-cellular calcium metabolism such as sacroplasmic/endoplasmic reticulum Ca^{2+}-ATPase (SERCA)-2 [30], Indeed, alterations in these cardiomyocyte-related processes are important molecular mechanisms underlying diastolic dysfunction [3]. Aforementioned fibrotic changes of the extracellular matrix of the myocardium relate to the stimulation of the TGF-β_1 pathway [17]. Angiotensin-II (Ang-II) is a potent inducer of the TGF-β_1 pathway directly and indirectly via stimulation of NAD(P)H oxidase and generation of superoxide anions, i.e. oxidative stress. Activation of neurohormonal systems such as RAAS and the endogenous endothelin system as well as reduction of the efficacy of the nitric oxide (NO) system have been discussed as additional factors in the pathophysiology of diastolic dysfunction [3], Upregulation of Ang-II, ET-1, and TGF-$\beta_{1,2}$ production along with

neovascularization and collagen production was demonstrated in coronary arteries in HC as well, highlighting intriguing parallels in the pathophysiology of cardiac and vascular changes under those pathophysiological conditions [11]. Taking our prior data on the alteration of myocardial perfusion and permeability in HC into consideration, one may wonder how much vascular and myocardial changes are intertwined functionally and causally [14], Intriguingly, in humans, impaired microvascular endothelial function and hyperlipidemia are equally associated with diastolic dysfunction [33], Taken together, diastolic dysfunction in HC is caused at least in part by the activation of neurohormonal systems and the generation of oxidative stress, which trigger the TGF-β_1 pathway, leading to increased collagen production and stiffening of the ventricle.

4.4. Stains and diastolic function

Introduced to interfere primarily with vascular changes, statins have been shown to improve cardiac abnormalities in ischemic and nonischemic cardiomyopathies with various degrees of systolic function impairment [34–36], Two non-randomized cohort studies in particular suggested that statins improve long-term survival of patients with heart failure and preserved systolic function [9,10], These benefits have been attributed to a decrease in neurohormonal activation and normalization of the sympathovagal balance in experimental models and has been furthermore related to a down-regulation of the expression of Ang-II type I receptors and NAD(P)H oxidase subunits in the central nervous system [37–39]., Preservation of eNOS expression and activity is another important mechanism that has been identified to account for the benefit of statins in heart failure, including inhibitory effects on cardiac hypertrophy [40,41], Of note, induction of the regression of cardiac hypertrophy and fibrosis were among the very first effects outlined for statins in ischemic and non-ischemic heart failure models and were related to the non-lipid-lowering effects, especially interference with the activation of Rho family members such as Racl and RhoA [42–44], Moreover, in experimental renovascular hypertension, simvastatin decreases RhoA and TGF-β expression and preserves myocardial eNOS expression along with anti-inflammatory, anti-angiogenic, and anti-fibrotic effects [32], Likewise in the current study, no changes in lipid serum concentrations or vital parameters were observed, yet simvastatin had a remarkable impact on myocardial microstructure and function. Simvastatin prevented not only myocardial neovascularization but, as an important new finding, collagen production and cross-linking mainly in the perivascular segments. This corresponded to an improvement in diastolic function parameters, pointing out the significance of this combined, angio-fibrotic remodeling process for cardiac function. On a molecular level, we noted a decrease in the expression of pro-angiogenic factors such as VEGF and bFGF and pro-fibrotic factors such TGF-β_1. While the expression of these factors is regulated by different transcription factors, a unifying factor might be oxidative stress. Indeed, in prior studies we were able to demonstrate strikingly similar results of reduction of myocardial neovascularization and perivascular fibrosis along with an improvement in diastolic function by antioxidant therapy alone [17,45], Furthermore, we were able to demonstrate before that simvastatin at the dose regimen used in the current study decreases tissue oxidative stress [12,46], Hence, via their non-lipid-lowering properties, statins decrease myocardial neovascularization, collagen deposition and cross-linking, i.e. myocardial fibrosis, which results in an improvement in diastolic function.

4.5. Study limitations

Even though used at a dose that would fall into the high-dose category in clinical practice, simvastatin at 80 mg per day did not lower cholesterol serum concentrations, either in this study or in a previous study with hypertensive female domestic pigs subjected to a normal diet [32]. Similarly, no lipid-lowering effects were observed in hypercholesterolemic Yucatan pigs receiving high-dose atorvastatin therapy over 20 weeks [47]. In fact, just like

in the current study, cholesterol serum concentrations were slightly higher in the statin-treated group, which, nevertheless, experienced improvement in microvascular vasoreactivity [47]. In diabetic dyslipidemic male Yucatan pigs, daily administration of 80 mg of atorvastatin reduced triglyceride but not LDL levels and still decreased vascular collagen deposition [48]. On the contrary, in familial hypercholesterolemic pigs, simvastatin did not reduce triglyceride but decreased LDL levels and the largest effect was noted at a daily dose of 200 mg [49]. Hence, the dose-response curve for statins with regards to lipid serum parameters differs between pigs and humans, and direct dose correlations are difficult to make. Consistent with other studies, however, the dose of simvastatin used in the current study would have to be considered to be in the low-dose category.

Despite the variation in the lipid-lowering response to statins, the non-lipid-lowering effects are universally present and relevant. For instance, even though pravastatin, contrary to atorvastatin, does not reduce non-HDL cholesterol serum concentrations in Yorkshire-Albino pigs fed a high-cholesterol diet for 8 weeks, both statins decrease the expression of pro-inflammatory molecules in different arterial beds too a similar extent [50]. Hence, the degree of lipid-lowering is not linearly linked to the extent of the non-lipid-lowering effects of statins. The current study highlights lipid-lowering-independent effects of statins on myocardial structure and function. As with other experimental studies, concerns regarding the translation into clinical practice are inherent. Nevertheless, experimental studies such as the current one point out principles with pathophysiological and therapeutic implications. Testing and translating these further is the objective of clinical studies. As such, the current study encourages randomized, dose-escalating, and placebo-controlled trials to validate the clinical merit of statin therapy in diastolic heart failure.

5. Conclusion

The current findings support the concept that HC contributes to diastolic dysfunction at least in part by promoting myocardial collagen deposition, noted in particular around an increased myocardial microvasculature. Interference with this process and reduction of myocardial fibrosis and angiogenesis rather than reduction of cholesterol serum levels seems to be a key element of the beneficial effects of statins on diastolic function.

Acknowledgments

This study was supported by the following NIH grants: K24, HL69840, HL-63911, DK73608, HL77131, and HL085307.

References

1. Zile MR, Brutsaert DL. New concepts in diastolic dysfunction and diastolic heart failure: part I: diagnosis, prognosis, and measurements of diastolic function. Circulation. 2002; 105:1387–93. [PubMed: 11901053]
2. Redfield MM, Jacobsen SJ, Burnett JC Jr, Mahoney DW, Bailey KR, Rodeheffer RJ. Burden of systolic and diastolic ventricular dysfunction in the community: appreciating the scope of the heart failure epidemic. JAMA. 2003; 289:194–202. [PubMed: 12517230]
3. Zile MR, Brutsaert DL. New concepts in diastolic dysfunction and diastolic heart failure: part II: causal mechanisms and treatment. Circulation. 2002; 105:1503–8. [PubMed: 11914262]
4. Brower GL, Gardner JD, Forman MF, et al. The relationship between myocardial extracellular matrix remodeling and ventricular function. Eur J Cardiothorac Surg. 2006; 30:604–10. [PubMed: 16935520]
5. Rosenkranz S. TGF-beta1 and angiotensin networking in cardiac remodeling. Cardiovasc Res. 2004; 63:423–32. [PubMed: 15276467]

6. Paulus WJ. The role of nitric oxide in the failing heart. Heart Fail Rev. 2001; 6:105–18. [PubMed: 11309529]
7. Bonetti PO, Lerman LO, Napoli C, Lerman A. Statin effects beyond lipid lowering—are they clinically relevant? Eur Heart J. 2003; 24:225–48. [PubMed: 12590901]
8. Takemoto M, Liao JK. Pleiotropic effects of 3-hydroxy-3-methylglutaryl coenzyme a reductase inhibitors. Arterioscler Thromb Vasc Biol. 2001; 21:1712–9. [PubMed: 11701455]
9. Fukuta H, Sane DC, Brucks S, Little WC. Statin therapy may be associated with lower mortality in patients with diastolic heart failure: a preliminary report. Circulation. 2005; 112:357–63. [PubMed: 16009792]
10. Shah R, Wang Y, Foody JM. Effect of statins, angiotensin-converting enzyme inhibitors, and beta blockers on survival in patients ≥65 years of age with heart failure and preserved left ventricular systolic function. Am J Cardiol. 2008; 101:217–22. [PubMed: 18178410]
11. Herrmann J, Samee S, Chade A, Rodriguez Porcel M, Lerman LO, Lerman A. Differential effect of experimental hypertension and hypercholesterolemia on adventitial remodeling. Arterioscler Thromb Vasc Biol. 2005; 25:447–53. [PubMed: 15591225]
12. Wilson SH, Simari RD, Best PJ, et al. Simvastatin preserves coronary endothelial function in hypercholesterolemia in the absence of lipid lowering. Arterioscler Thromb Vasc Biol. 2001; 21:122–8. [PubMed: 11145943]
13. Wilson SH, Herrmann J, Lerman LO, et al. Simvastatin preserves the structure of coronary adventitial vasa vasorum in experimental hypercholesterolemia independent of lipid lowering. Circulation. 2002; 105:415–8. [PubMed: 11815421]
14. Bonetti PO, Wilson SH, Rodriguez-Porcel M, Holmes DR Jr, Lerman LO, Lerman A. Simvastatin preserves myocardial perfusion and coronary microvascular permeability in experimental hypercholesterolemia independent of lipid lowering. J Am Coll Cardiol. 2002; 40:546–54. [PubMed: 12142124]
15. Rodriguez-Porcel M, Lerman A, Ritman EL, Wilson SH, Best PJ, Lerman LO. Altered myocardial microvascular 3D architecture in experimental hypercholesterolemia. Circulation. 2000; 102:2028–30. [PubMed: 11044415]
16. Rodriguez-Porcel M, Zhu XY, Chade AR, et al. Functional and structural remodeling of the myocardial microvasculature in early experimental hypertension. Am J Physiol Heart Circ Physiol. 2006; 290:H978–84. [PubMed: 16214846]
17. Zhu XY, Daghini E, Rodriguez-Porcel M, et al. Redox-sensitive myocardial remodeling and dysfunction in swine diet-induced experimental hypercholes-terolemia. Atherosclerosis. 2007; 193:62–9. [PubMed: 16996066]
18. Rumberger JA. Use of electron beam tomography to quantify cardiac diastolic function. Cardiol Clin. 2000; 18:547–56. [PubMed: 10986588]
19. Crisby M, Nordin-Fredriksson G, Shah PK, Yano J, Zhu J, Nilsson J. Pravastatin treatment increases collagen content and decreases lipid content, inflammation, metalloproteinases, and cell death in human carotid plaques:implications for plaque stabilization. Circulation. 2001; 103:926–33. [PubMed: 11181465]
20. Stegemann H, Stalder K. Determination of hydroxyproline. Clin Chim Acta. 1967; 18:267–73. [PubMed: 4864804]
21. Miller EJ, Rhodes RK. Preparation and characterization of the different types of collagen. Methods Enzymol. 1982:82, 33–64. Pt A. [PubMed: 6218378]
22. Mandinov L, Eberli FR, Seiler C, Hess OM. Diastolic heart failure. Cardiovasc Res. 2000; 45:813–25. [PubMed: 10728407]
23. Daghini E, Ritman EL, Lerman LO. Examine thy heart with all diligence: evaluation of cardiac function using fast computed tomography. Hypertension. 2007; 49:249–56. [PubMed: 17159086]
24. Thomson HL, Basmadjian AJ, Rainbird AJ, et al. Contrast echocardiography improves the accuracy and reproducibility of left ventricular remodeling measurements: a prospective, randomly assigned, blinded study. J Am Coll Cardiol. 2001; 38:867–75. [PubMed: 11527647]
25. Rumberger JA, Weiss RM, Feiring AJ, et al. Patterns of regional diastolic function in the normal human left ventricle: an ultrafast computed tomographic study. J Am Coll Cardiol. 1989; 14:119–26. [PubMed: 2738256]

26. Lerman LO, Siripornpitak S, Maffei NL, Sheedy PF 2nd, Ritman EL. Measurement of in vivo myocardial microcirculatory function with electron beam CT. J Comput Assist Tomogr. 1999; 23:390–8. [PubMed: 10348445]
27. Daghini E, Primak AN, Chade AR, et al. Evaluation of porcine myocardial microvascular permeability and fractional vascular volume using 64-slice helical computed tomography (CT). Invest Radiol. 2007; 42:274–82. [PubMed: 17414522]
28. Palmiero P, Maiello M, Passantino A, et al. Correlation between diastolicimpairment and lipid metabolism in mild-to-moderate hypertensive postmenopausal women. Am J Hypertens. 2002; 15:615–20. [PubMed: 12118909]
29. Salmasi AM, Frost P, Dancy M. Impaired left ventricular diastolic function during isometric exercise in asymptomatic patients with hyperlipidaemia. Int J Cardiol. 2004; 95:275–80. [PubMed: 15193832]
30. Huang Y, Walker KE, Hanley F, Narula J, Houser SR, Tulenko TN. Cardiac systolic and diastolic dysfunction after a cholesterol-rich diet. Circulation. 2004; 109:97–102. [PubMed: 14676147]
31. Norton GR, Tsotetsi J, Trifunovic B, Hartford C, Candy GP, Woodiwiss AJ. Myocardial stiffness is attributed to alterations in cross-linked collagen rather than total collagen or phenotypes in spontaneously hypertensive rats. Circulation. 1997; 96:1991–8. [PubMed: 9323091]
32. Zhu XY, Daghini E, Chade AR, et al. Simvastatin prevents coronary microvascular remodeling in renovascular hypertensive pigs. J Am Soc Nephrol. 2007; 18:1209–17. [PubMed: 17344424]
33. Elesber AA, Redfield MM, Rihal CS, et al. Coronary endothelial dysfunction and hyperlipidemia are independently associated with diastolic dysfunction in humans. Am Heart J. 2007; 153:1081–107. [PubMed: 17540214]
34. Foody JM, Shah R, Galusha D, Masoudi FA, Havranek EP, Krumholz HM. Statins and mortality among elderly patients hospitalized with heart failure. Circulation. 2006; 113:1086–92. [PubMed: 16490817]
35. Go AS, Lee WY, Yang J, Lo JC, Gurwitz JH. Statin therapy and risks for death and hospitalization in chronic heart failure. JAMA. 2006; 296:2105–11. [PubMed: 17077375]
36. Ramasubbu K, Estep J, White DL, Deswal A, Mann DL. Experimental and clinical basis for the use of statins in patients with ischemic and nonischemic cardiomyopathy. J Am Coll Cardiol. 2008; 51:415–26. [PubMed: 18222351]
37. Pliquett RU, Cornish KG, Peuler JD, Zucker IH. Simvastatin normalizes autonomic neural control in experimental heart failure. Circulation. 2003; 107:2493–8. [PubMed: 12695293]
38. Pliquett RU, Cornish KG, Zucker IH. Statin therapy restores sympathovagal balance in experimental heart failure. J Appl Physiol. 2003; 95:700–4. [PubMed: 12716869]
39. Gao L, Wang W, Li YL, et al. Simvastatin therapy normalizes sympathetic neural control in experimental heart failure: roles of angiotensin II type 1 receptors and NAD(P)H oxidase. Circulation. 2005; 112:1763–70. [PubMed: 16157767]
40. Trochu JN, Mital S, Zhang X, et al. Preservation of NO production by statins in the treatment of heart failure. Cardiovasc Res. 2003; 60:250–8. [PubMed: 14613854]
41. Greer JJ, Kakkar AK, Elrod JW, Watson LJ, Jones SP, Lefer DJ. Low-dose simvastatin improves survival and ventricular function via eNOS in congestive heart failure. Am J Physiol Heart Circ Physiol. 2006; 291:H2743–51. [PubMed: 16844920]
42. Patel R, Nagueh SF, Tsybouleva N, et al. Simvastatin induces regression of cardiac hypertrophy and fibrosis and improves cardiac function in a transgenic rabbit model of human hypertrophic cardiomyopathy. Circulation. 2001; 104:317–24. [PubMed: 11457751]
43. Hayashidani S, Tsutsui H, Shiomi T, et al. Fluvastatin, a 3-hydroxy-3-methylglutaryl coenzyme a reductase inhibitor, attenuates left ventricular remodeling and failure after experimental myocardial infarction. Circulation. 2002; 105:868–73. [PubMed: 11854129]
44. Nakagami H, Jensen KS, Liao JK. A novel pleiotropic effect of statins: prevention of cardiac hypertrophy by cholesterol-independent mechanisms. Ann Med. 2003; 35:398–403. [PubMed: 14572163]
45. Zhu XY, Rodriguez-Porcel M, Bentley MD, et al. Antioxidant intervention attenuates myocardial neovascularization in hypercholesterolemia. Circulation. 2004; 109:2109–15. [PubMed: 15051643]

46. Wilson SH, Chade AR, Feldstein A, et al. Lipid-lowering-independent effects of simvastatin on the kidney in experimental hypercholesterolaemia. Nephrol Dial Transplant. 2003; 18:703–9. [PubMed: 12637638]

47. Boodhwani M, Nakai Y, Voisine P, et al. High-dose atorvastatin improves hypercholesterolemic coronary endothelial dysfunction with out improving the angiogenic response. Circulation. 2006; 114:I402–8. [PubMed: 16820608]

48. Dixon JL, Shen S, Vuchetich JP, Wysocka E, Sun GY, Sturek M. Increased atherosclerosis in diabetic dyslipidemic swine: protection by atorvastatin involves decreased VLDL triglycerides but minimal effects on the lipoprotein profile. J Lipid Res. 2002; 43:1618–29. [PubMed: 12364546]

49. Hasler-Rapacz J, Kempen HJ, Princen HM, Kudchodkar BJ, Lacko A, Rapacz J. Effects of simvastatin on plasma lipids and apolipoproteins in familial hypercholesterolemic swine. Arterioscler Thromb Vasc Biol. 1996; 16:137–43. [PubMed: 8548414]

50. Martinez-Gonzalez J, Alfon J, Berrozpe M, Badimon L. HMG-CoA reductase inhibitors reduce vascular monocyte chemotactic protein-1expression in early lesions from hypercholesterolemic swine independently of their effect on plasma cholesterol levels. Atherosclerosis. 2001; 159:27–33. [PubMed: 11689203]

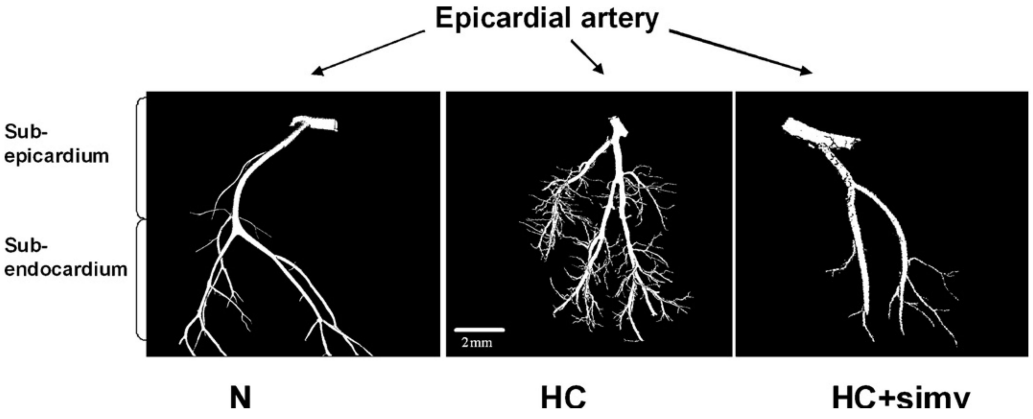

Fig. 1.

Micro-CT imaging of topographically isolated coronary arteries and their myocardial branches highlighting an increase in small tortuous vessels in the myocardium of animals on a high-cholesterol diet (HC) for 12 weeks compared with those on a normal diet (N), which was prevented by concomitant simvastatin treatment (HC + simv); voxel size 20 μm.

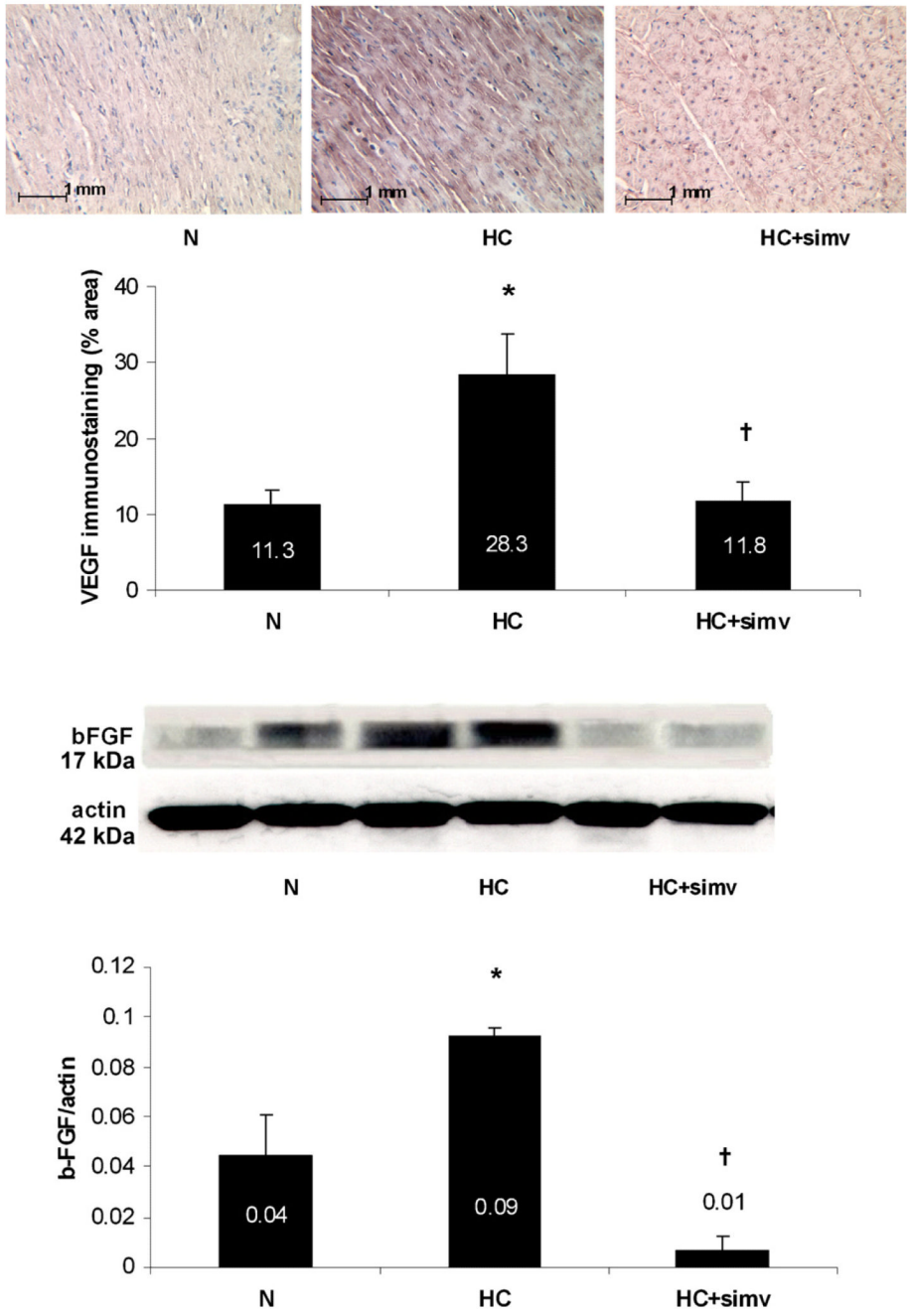

Fig. 2.

(Top panel) Representative immunostaining for VEGF-A of the myocardium from animals on a normal diet (N), a high-cholesterol diet (HC), and a high-cholesterol diet with simvastatin (HC + simv) for 12 weeks. Positive staining is displayed in red, magnification ×20. Bar graph illustrates the percentage of positive immunoreactivity per myocardial area averaged for 18 myocardial slides per group; values are expressed as mean ± SEM, $*p < 0.05$ compared to animals on a normal diet, $\dagger p < 0.05$ compared to animals on a high-cholesterol diet. (Bottom panel) Representative immunoblot for myocardial b-FGF expression with two lanes per study group as defined above. Bar graph illustrates the expression as a densitometric ratio to β-actin averaged for 6 samples per group; values are

expressed as mean ± SEM, *$p < 0.05$ compared to animals on a normal diet, †$p < 0.05$ compared to animals on a high-cholesterol diet. (For interpretation of the references to color in this figure legend, the reader is referred to the web version of the article.)

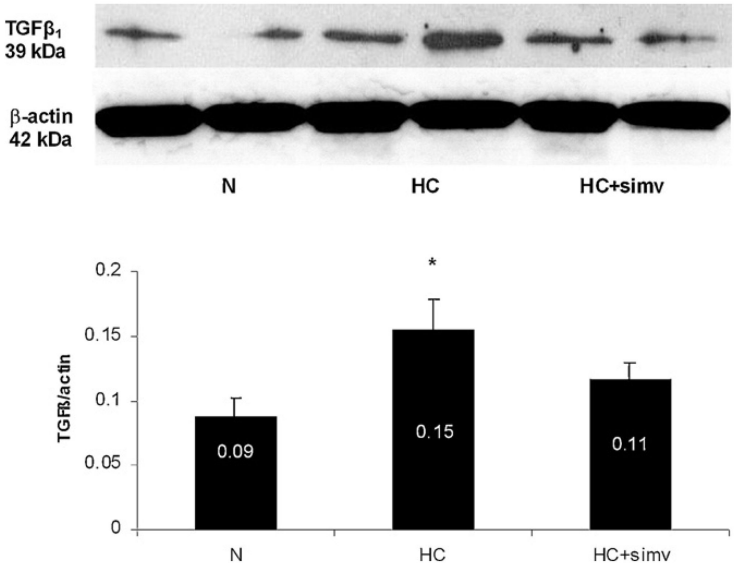

Fig. 3.

Representative immunoblot for TGFβ_1 expression in the myocardium of animals on a normal diet (N), a high-cholesterol diet (HC), and a high-cholesterol diet with simvastatin (HC + simv) for 12 weeks. Bar graph illustrates the expression as a densitometric ratio to β-actin averaged for 6 samples per group; values are expressed as mean ± SEM, *$p < 0.05$ compared to animals on a normal diet.

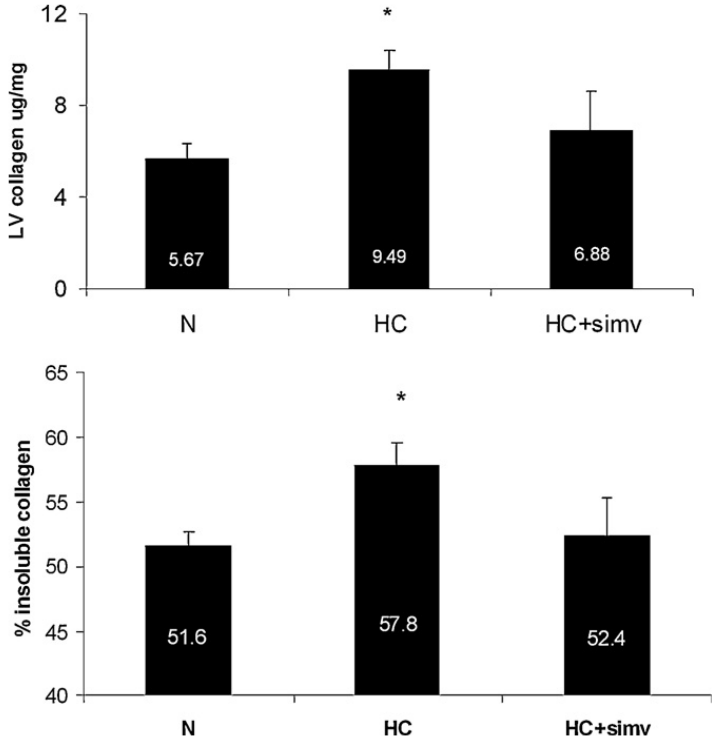

Fig. 4.

(Top panel) Total collagen content quantified by measuring hydroxyproline in the myocardium of animals on a normal diet (N), a high-cholesterol diet (HC), and high-cholesterol diet with simvastatin (HC + simv) for 12 weeks. Bar graph illustrates total collagen content in microgram per milligram myocardial tissue in the three study group, averaged for 8 samples in N and HC group and 3 samples in HC + simv group; values are expressed as mean ± SEM, $*p < 0.05$ compared to animals on a normal diet. (Bottom panel) Content of insoluble (cross-linked) collagen in the myocardium of animals of the three study groups. Bar graph illustrates the fraction of insoluble collagen among the total amount of collagen in the three group as detailed above; values are expressed as mean ± SEM, $*p < 0.05$ compared to animals on a normal diet.

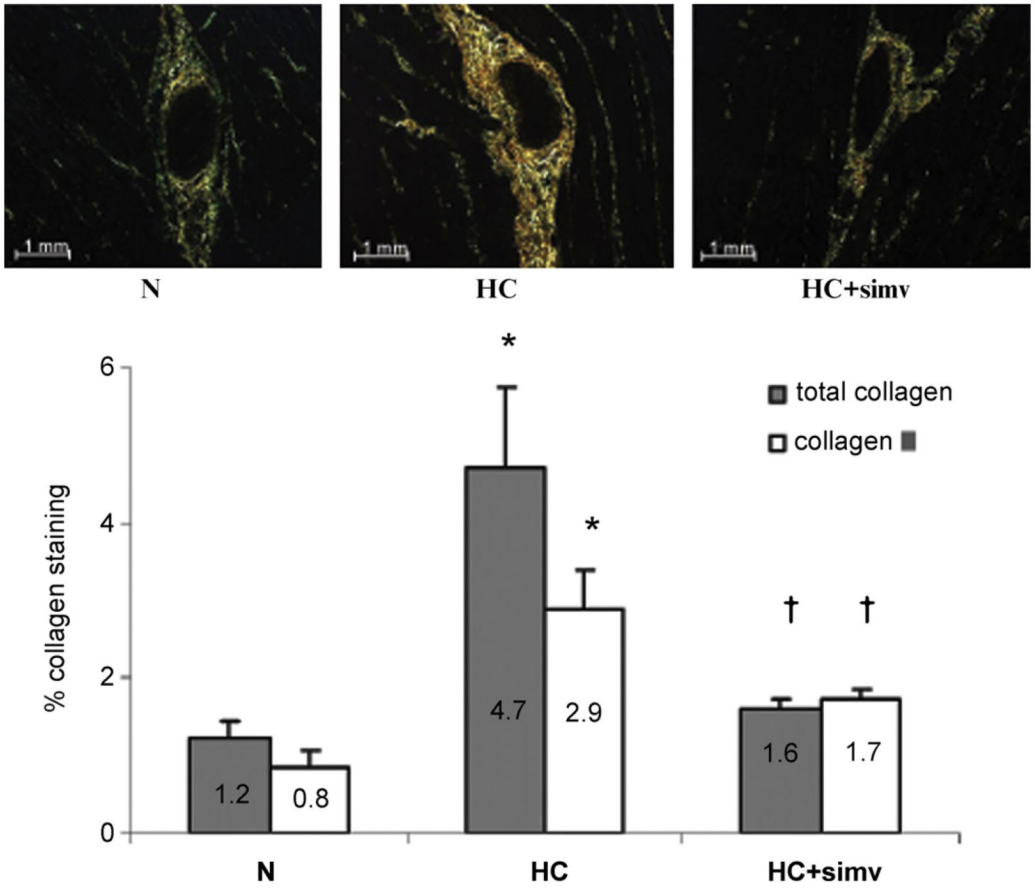

Fig. 5.

(Top panel) Sirius-red staining of myocardium from animals on a normal diet (N), a high-cholesterol diet (HC), and a high-cholesterol diet with simvastatin (HC + simv) for 12 weeks, viewed under polarized light, magnification × 20. Collagen I appears red/orange while collage III is yellow/green. As readily notable, both are prominently present in perivascular matrix of the myocardium of HC animals. (Bottom panel) Bar graph illustrates the percentage of total collagen and collagen III per myocardial area in the three study groups, averaged for 6 samples in N, 5 samples in HC, and 4 samples in HC + simv group; values as mean ± SEM, *$p < 0.05$ compared to animals on a normal diet, †$p < 0.05$ compared to animals on a high-cholesterol diet. (For interpretation of the references to color in this figure legend, the reader is referred to the web version of the article.)

Table 1

Hemodynamics parameters and plasma lipid profile in the different study groups.

	Normal diet	High-cholesterol diet	High-cholesterol diet + simvastatin
Left ventricular muscle mass, g	105.3 ± 3.1	110.0 ± 3.6	105.8 ± 4.3
Diastolic filling rate, mL/s	151.1 ± 12.1	102.4 ± 11.3*	176.8 ± 21.3†
Ejection fraction, %	55 ± 2	59 ± 1	58 ± 1
Cardiac output, L/min	4.4 ± 0.2	4.2 ± 0.5	4.6 ± 0.6
Systemic vascular resistance, dyn s^{-1} cm^{-5}	26.8 ± 1.3	27.0 ± 4.1	25.9 ± 4.7
Myocardial vascular resistance			
Baseline, dyn s^{-1} cm^{-5}	97.2 ± 7.9	82.2 ± 9.0	91.2 ± 9.1
Adenosine, % change	−37.7 ± 5.1	−3.7 ± 8.2*	−33.4 ± 7.5†
Mean arterial pressure			
Baseline, mmHg	117 ± 5	109 ± 8	102 ± 4
Adenosine, % change	−11 ± 3	−18 ± 5	−12 ± 3
Heart rate			
Baseline, beats/min	74 ± 3	70 ± 5	79 ± 7
Adenosine, % change	9 ± 9	7 ± 5	12 ± 2
Lipid profile, mmol/L			
Total cholesterol	2.1 ± 0.1	10.7 ± 1.8*	12.4 ± 1.4*
Low density lipoprotein	1.0 ± 0.1	7.9 ± 1.7*	9.6 ± 1.2*
High density lipoprotein	1.0 ± 0.3	2.6 ± 0.3*	2.6 ± 0.2*
Triglycerides	0.29 ± 0.05	0.40 ± 0.06	0.28 ± 0.04

Values are expressed as mean±SEM of experiments performed in 6 animals per group.

*$p < 0.05$ compared to normal diet animals.

†$p < 0.05$ compared to high-cholesterol diet animals.

Table 2

Microvessel count and volume fraction in the different study groups.

	Normal diet	High-cholesterol diet	High-cholesterol diet + simvastatin
Subepicardial vessel count [*n*]			
Small (≤100μm)	86 ± 36	317 ± 17 *	172 ± 48 †
Large (101−500μm)	23 ± 8	32 ± 7	17 ± 7
Subendocardial vessel count [n]			
Small (≤100μm)	117 ± 39	350 ± 42 *	249 ± 37
Large (101−500μm)	31 ± 10	26 ± 3	22 ± 7
Vascular fraction, %	1.98 ± 0.84	4.48 ± 0.31 *	2.95 ± 0.29

Values are expressed as mean±SEM of experiments performed in 6 animals per group.

* $p < 0.05$ compared to normal diet animals.

† $p < 0.05$ compared to high-cholesterol diet animals.